Search for Pulsed TeV Gamma-Ray Emission from Young Pulsars with H.E.S.S.

F. Schmidt*, F. Breitling*, S. Gillessen†, A. Konopelko*†, T. Lohse*, S. Schlenker*, U. Schwanke* and C. Stegmann*
for the H.E.S.S. collaboration

*Institut für Physik, Humboldt-Universität zu Berlin, Newtonstr. 15, D-12489 Berlin, Germany
†Max-Planck-Institut für Kernphysik, P.O. Box 103980, D-69029 Heidelberg, Germany

Abstract. The H.E.S.S. experiment is a next-generation imaging atmospheric Cherenkov detector with a ∼1% Crab flux sensitivity for gamma-rays above 100 GeV. The full 4-telescope array has been operational since December 2003. The three young pulsars, Crab, Vela, and PSR B1706-44, are among the six pulsars whose pulsed emission has been detected up to energies of several GeV by EGRET. These pulsars have been selected for H.E.S.S. observations on grounds of their high rank in apparent spin-down luminosity $\dot{E}_{sd}/d^2$ and observability for the H.E.S.S. array. No pulsed emission was found and flux upper limits are given.

INTRODUCTION

Up to now, high-energy emission from pulsars is observed from the optical through X-ray up to the GeV gamma range. A significant fraction of the spin-down power of the gamma-ray emitting pulsars is radiated in this range. Physical parameters including the period P, distance d, surface magnetic field B_s and spin-down luminosity $\dot{E}_{sd}$, of the observed pulsars are summarized in Table 1. The high-energy radiation is commonly assumed to be produced by electrons and positrons accelerated in the vicinity of the rotating neutron star, in the so-called pulsar magnetosphere. The primary accelerated particles emit synchrotron and curvature radiation, inducing electromagnetic cascades via pair production mechanisms. TeV Gamma-rays might also be produced by the energetic particles via inverse Compton scattering off soft photons.

There is no consensus on the location of the accelerating regions in the magnetosphere. Two scenarios are especially popular: the *polar cap* model places the acceleration zone near the neutron star surface at the magnetic pole, the *outer gap* model assumes an extended acceleration region along the last open magnetic field lines. Observations at the highest energies are crucial for distinguishing between these models, as the radiation of the primary particles can be observed directly in this range.

The H.E.S.S. experiment [1] is an atmospheric Cherenkov detector dedicated to the observation of gamma-rays with energies above 100 GeV. Situated in Namibia, the full 4-telescope array has been operational since December 2003. Each telescope has a mirror area of 107 m^2 and is equipped with a camera consisting of 960 photomultiplier tubes. The system has a field of view of 5° and allows a reconstruction of the individual shower direction and energy, with precisions of 0.1° and approximately 15%.

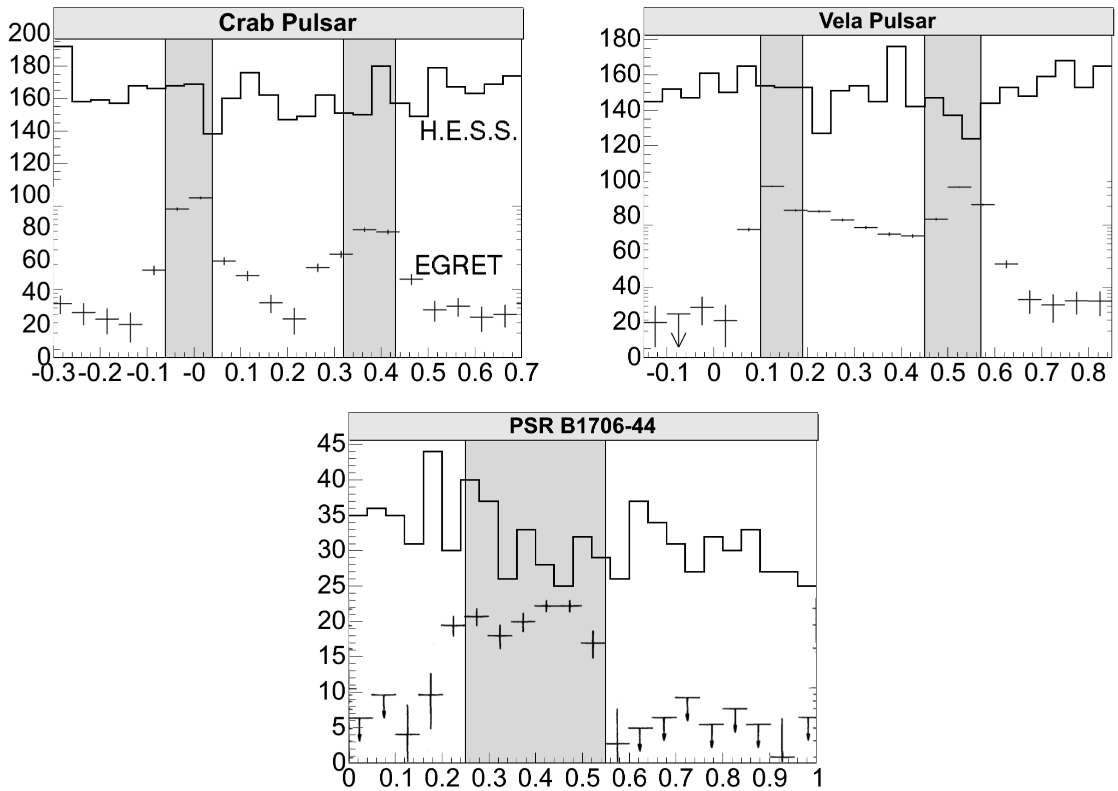

FIGURE 1. Phasograms (total count of events passing all cuts, binned in pulsar phase) for the three observed pulsars; EGRET pulse profi les (crosses, [3, 4]) and signal regions (shaded areas) are indicated.

TABLE 1. Physical parameters of the observed pulsars.

	P **[ms]**	d **[kpc]**	B_s [10^{12} **G]**	$\dot{E}_{sd}$ **[erg s^{-1}]**
Crab	33.4	2.0	3.7	$4.5 \cdot 10^{38}$
Vela	89.3	0.3	3.3	$6.9 \cdot 10^{36}$
PSR B1706-44	102.4	1.8	3.1	$3.4 \cdot 10^{36}$

DATA ANALYSIS AND RESULTS

The data sets used for the analysis were recorded from April to July 2003 (for PSR B1706−44), in October 2003 (for Crab), and January to March 2004 (for Vela). Only runs fulfilling strict quality criteria were selected. During the first period, two of four telescopes were operational and events were combined in software. From October 2003 on, data were taken with three or four telescopes and an array-level hardware trigger [2]. The configurations and live times are summarized in Table 2.

After calibration and image cleaning, showers were reconstructed using standard techniques [5, 6]. Cuts were applied on image parameters such as scaled width, scaled length and image amplitude, as well as on the reconstructed shower direction in order to reduce the hadronic background [5].

TABLE 2. Summary of data sets and results.

	Crab	**Vela**	**PSR B1706-44**
Confi guration	3 Tel.	3/4 Tel.	2 Tel. (no central trigger)
Live time	4.0 h	12.8 h	14.3 h
Phase regions	$[0.94, 0.04] \cup$ $[0.32, 0.43]$	$[0.1, 0.19] \cup$ $[0.45, 0.57]$	$[0.15, 0.55]$
Integr. flux upper limit* $[10^{-12}\,\mathrm{cm}^{-2}\mathrm{s}^{-1}]$	6.30 (> 560 GeV) 2.79 (> 1 TeV)	0.50 (> 400 GeV) 0.22 (> 1 TeV)	1.38 (> 500 GeV) 0.49 (> 1 TeV)

* 99.9% confi dence level

TABLE 3. Upper limits on pulsed emission relative to DC flux for the **Crab pulsar**.

Energy range	**Relative upper limit (99.9% confidence level)**	**Upper limit* on** dN/dE
< 500 GeV	3.7 %	$1.1 \cdot 10^{-11}\,\mathrm{cm}^{-2}\,\mathrm{s}^{-1}\,\mathrm{TeV}^{-1}$
0.5...1 TeV	3.4 %	$2.7 \cdot 10^{-12}\,\mathrm{cm}^{-2}\,\mathrm{s}^{-1}\,\mathrm{TeV}^{-1}$
> 1 TeV	6.0 %	$1.4 \cdot 10^{-13}\,\mathrm{cm}^{-2}\,\mathrm{s}^{-1}\,\mathrm{TeV}^{-1}$

* Using DC spectrum from [10].

The GPS time stamps of the events which passed the gamma-candidate selection were transformed to the solar system barycenter via the DE200 ephemerides [7]. Using radio ephemerides of the observed pulsars from Jodrell Bank[1] and the Australian Pulsar Timing Archive[2], the events are folded into a phase histogram ("phasogram"). The phasograms for the three pulsars are shown in Figure 1, which show no signal modulated at the pulsar frequency. Figure 1 also shows the EGRET pulse profiles taken from [3, 4].

We take the observed EGRET pulse regions in the phasograms (indicated in Figure 1) as signal regions for the upper limit calculation. The remainder of the respective phasogram is considered as background. Using the Helene method [8] and effective collection areas derived from Monte Carlo simulations, upper limits on the flux were calculated to a confidence level of 99.9%. Details on the model-independent upper limit calculation for the integrated flux can be found in [9]. The derived integrated flux upper limits are summarized in Table 2.

For the Crab pulsar, it is possible to determine relative upper limits on the pulsed emission with respect to the observed DC flux, assuming the pulsed emission has the same spectrum as the unpulsed one (Table 3). The systematic uncertainties involved in determining the effective collection areas are thus reduced.

The upper limit on the fraction of pulsed emission is the ratio of the upper limit on

---

[1] See `http://www.jb.man.ac.uk/~pulsar/crab.html`
[2] See `http://www.atnf.csiro.au/research/pulsar/archive/`

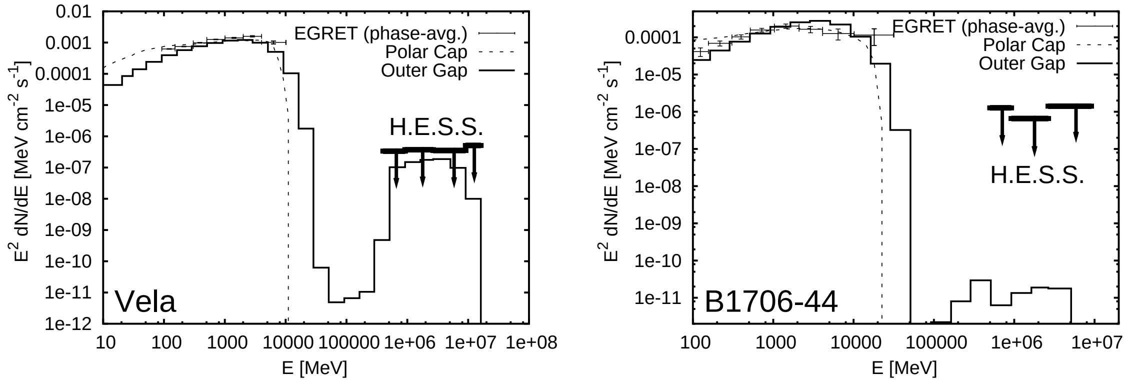

FIGURE 2. Pulsar model spectra for Vela and PSR B1706-44 with EGRET phase-averaged data points [3, 4] and H.E.S.S. upper limits.

the number of events in the phasogram due to a pulsed component, which is determined from the excess of the signal region over the background region in the phasogram, to the normalized DC excess in the background region of the phasogram, which is derived from on- and off-source areas in the field of view. This can be converted into an absolute flux upper limit using the known DC spectrum of the Crab nebula [10].

Using the reconstructed shower energy one can also derive energy-resolved differential flux upper limits in energy bins in a similar way as the integrated flux upper limits. These upper limits, shown in Figure 2 for the Vela pulsar and PSR B1706-44, are independent of any model assumptions. Also shown in Figure 2 are model predictions which were calculated in the framework of recent *polar cap* [11, 12] and *outer gap* [13] models. In the near future, improved upper limits will further constrain pulsar models in this energy range. For all upper limits, the lower energy bound was chosen such that the correction for biases in the energy reconstruction stayed lower than 10%.

SUMMARY

H.E.S.S. observations of the three young pulsars, Crab, Vela, and PSR B1706-44, reveal no indication of a pulsed signal above a few hundred GeV. The derived flux upper limits are considerably lower than previous published upper limits in the case of Vela [14] and PSR B1706-44 [15]. In the near future, the upper limits will be improved by a careful treatment of the energy bias and analysis of additional recent observational data, putting further constraints on pulsar models. The presented results are preliminary, and no systematic errors are included yet.

ACKNOWLEDGMENTS

We would like to thank K. Hirotani and B. Rudak for kindly giving us access to simulation code which enabled us to compare our results with model predictions. Many thanks also go to the Jodrell Bank Pulsar Group, the Australian Pulsar Timing Archive, and Richard Dodson of the University of Tasmania for providing the pulsar ephemerides.

The support of the Namibian authorities and of the University of Namibia in facilitating the construction and operation of H.E.S.S. is gratefully acknowledged, as is the support by the German Ministry for Education and Research (BMBF), the Max Planck Society, the French Ministry for Research, the CNRS-IN2P3 and the Astroparticle Interdisciplinary Programme of the CNRS, the U.K. Particle Physics and Astronomy Research Council (PPARC), the IPNP of the Charles University, the South African Department of Science and Technology and National Research Foundation, and by the University of Namibia. We appreciate the excellent work of the technical support staff in Berlin, Durham, Hamburg, Heidelberg, Palaiseau, Paris, Saclay, and in Namibia in the construction and operation of the equipment.

REFERENCES

1. Hinton, J. A., *New Astronomy Reviews*, **48**, 331 (2004).
2. Funk, S. et al., *submitted to Astropart. Phys.* (2004).
3. Fierro, et al., *ApJ*, **494**, 734 (1998).
4. Thompson, D. J., et al., *ApJ*, **465**, 385 (1996).
5. Aharonian, F. et al. (H.E.S.S. collaboration), *submitted to A&A* (2004).
6. Aharonian, F. et al., *A&A*, **349**, 11 (1999).
7. Standish, E. M., *A&A*, **114**, 297 (1982).
8. Helene, O., *NIM*, **212**, 319 (1983).
9. Khelifi , B. et al., "Search for TeV Emission from the Direction of the Vela and PSR B1706-44 Pulsars," in *these proceedings*, 2004.
10. Aharonian, F. et al., *ApJ*, **539**, 317 (2000).
11. Daugherty, J. K., and Harding, A. K., *ApJ*, **252**, 337 (1982).
12. Rudak, B., and Dyks, J., *MNRAS*, **303**, 477 (1999).
13. Hirotani, K., "High-Energy Emission from Pulsar Outer Magnetospheres," in *Progress in Astrophysics Researches Vol. 1*, Nova Science Publishers, Hauppauge, NY, 2003, astro-ph/0307236.
14. Yoshikoshi, T. et al., *ApJ*, **487**, L65 (1997).
15. Chadwick, P. M. et al., *Astroparticle Physics*, **9**, 131 (1998).